

LNF-97/019

**Electronic Structure and Final–State Effects in  
Nd<sub>2</sub>CuO<sub>4</sub>, La<sub>2</sub>CuO<sub>4</sub>, and Ca<sub>2</sub>CuO<sub>3</sub> Compounds  
by Multiple–Scattering Theory at the  
Copper K Edge**

Ziyu Wu, M. Benfatto, C.R. Natoli

*Physical Review B Vol. 54, n. 19, 13 409–13 412, (1996)*

## Electronic structure and final-state effects in $\text{Nd}_2\text{CuO}_4$ , $\text{La}_2\text{CuO}_4$ , and $\text{Ca}_2\text{CuO}_3$ compounds by multichannel multiple-scattering theory at the copper $K$ edge

Ziyu Wu

*Institut des Matériaux de Nantes, Centre National de la Recherche Scientifique, UMR 110, Laboratoire de Chimie des Solides, 2 rue de la Houssinière, 44072 Nantes Cedex 03, France*

M. Benfatto and C. R. Natoli

*Istituto Nazionale di Fisica Nucleare, Laboratori Nazionali di Frascati, P.O. Box 13, 00044 Frascati, Italy*

(Received 8 November 1995; revised manuscript received 12 March 1996)

We present a theoretical analysis, based on the zeroth-order approximation of the multichannel multiple-scattering theory, of the x-ray-absorption spectra of  $\text{Nd}_2\text{CuO}_4$ ,  $\text{La}_2\text{CuO}_4$ , and  $\text{Ca}_2\text{CuO}_3$  compounds at the copper  $K$  edge. Single-channel theoretical calculations have been made using atomic clusters large enough to be sure that all one-electron features have been correctly described. On this basis the presence of both  $3d^9$  and  $3d^{10}\underline{L}$  configurations in the ground state has been found essential to obtain good agreement between experimental data and theoretical calculations in the case of  $\text{Nd}_2\text{CuO}_4$  and  $\text{Ca}_2\text{CuO}_3$ . Conversely, the best agreement with the  $\text{La}_2\text{CuO}_4$  data has been obtained by taking into account only the  $3d^{10}\underline{L}$  configuration in the final state. We briefly comment on this finding. [S0163-1829(96)02540-4]

Recently, there has been increasing interest in the electronic structure of  $\text{Nd}_2\text{CuO}_4$ ,  $\text{La}_2\text{CuO}_4$ , and  $\text{Ca}_2\text{CuO}_3$  compounds due to their structural and electronic similarity with high- $T_c$  superconductors. Important information obtained by x-ray-absorption spectroscopy (XAS) at the various edges<sup>1-20</sup> has led to useful insight into the chemical and electronic structure of these compounds, although there is still some debate<sup>9</sup> about their interpretation.

The Cu  $K$  edge is an interesting edge to investigate due to the possibility of obtaining relevant electronic and structural information about copper and its neighbors. At this edge the x-ray-absorption near edge structure (XANES) of  $\text{Nd}_2\text{CuO}_4$ ,  $\text{La}_2\text{CuO}_4$ , and  $\text{Ca}_2\text{CuO}_3$  show two sets of two peaks separated by about 7 eV.<sup>8-10</sup> These are shown as features  $A$  and  $A'$  for the first set, and features  $B$  and  $B'$  for the second set in Fig. 1, which is taken from the paper by Kosugi *et al.*<sup>9</sup> and reproduced here for the convenience of the reader. The interpretation proposed in Ref. 9 is that the two peaks in each set are replicas of the same one-electron transition originated by the presence of a poorly screened  $3d^9$  and a well-screened  $3d^{10}\underline{L}$  ( $\underline{L}$  denoting a hole in ligand oxygen) final-state electronic configuration in the presence of the core hole, while the two sets originate from  $1s \rightarrow p\sigma$  and  $1s \rightarrow p\pi$  one-electron transitions, representing in-plane and out-of-plane first coordination shell multiple-scattering features, in keeping with the divalent Cu valence state. In turn these two configurations are the relaxed counterpart, in the presence of the core hole, of the same two electronic configurations present in the ground state, where they are separated by about 2.5 eV (as we have calculated, the exact value depending on the different compound), the  $3d^9$  being lower than the  $3d^{10}\underline{L}$ . In the final state, instead, the presence of the core hole shifts the  $3d^{10}\underline{L}$  electronic configuration to lower energy than  $3d^9$ , due to the Coulomb interaction between the core hole and the quasilocalized  $d$  electrons, giving rise to a final state with a dominant  $3d^{10}\underline{L}$  character. The XAS spec-

trum could reflect the presence of these two electronic configurations by displaying particular features that cannot be assigned to one-electron transitions. Moreover, by just looking at the spectra, we propose the presence of a third set of twin features, labeled as  $C$  and  $C'$  in Fig. 1, in which the one-electron transition corresponds to multiple scattering of the final-state photoelectron within the first and second coordination shells.

In this paper we present a detailed theoretical study of the XANES spectra at Cu  $K$  edge of these materials based on the multichannel multiple-scattering (MCMS) theory<sup>21-23</sup> using large atomic clusters around the absorber, in the sense illustrated below, and the self-consistent-field (SCF) potential and charge densities following a method described in a previous work.<sup>24</sup> This method automatically takes into account the charge relaxation around the core hole. The radial extension of the clusters used in the calculations corresponds to a distance between the photoabsorber and the last neighbor of the same order of the photoelectron mean free path value, which is about 5–6 Å at the rising edge, taking into account only core-hole lifetime and experimental resolution, and even less at higher energies if one takes into account the photoelectron damping. We have verified that an increase of the cluster dimensions does not change significantly the shape of the theoretical spectra. On the basis of MCMS theory, assuming a final state formed by two electronic configurations, the total absorption cross section can be written<sup>21,23</sup> as

$$\sigma(\omega) = a_f^2 \sigma_0(k_0) + b_f^2 \sigma_1(k_1), \quad (1)$$

where  $\sigma_0(k_0)$  and  $\sigma_1(k_1)$  are the partial cross sections corresponding to  $3d^{10}\underline{L}$  and  $3d^9$  configurations, with wave vectors given by  $k_0^2 = \hbar\omega - I_c$  and  $k_1^2 = \hbar\omega - I_c - \Delta E$ , respectively. The coefficients  $a_f$  and  $b_f$  are the weight of the two configurations in the final state,  $I_c$  is the photoemission binding energy, and  $\Delta E$  is the energy splitting between the two

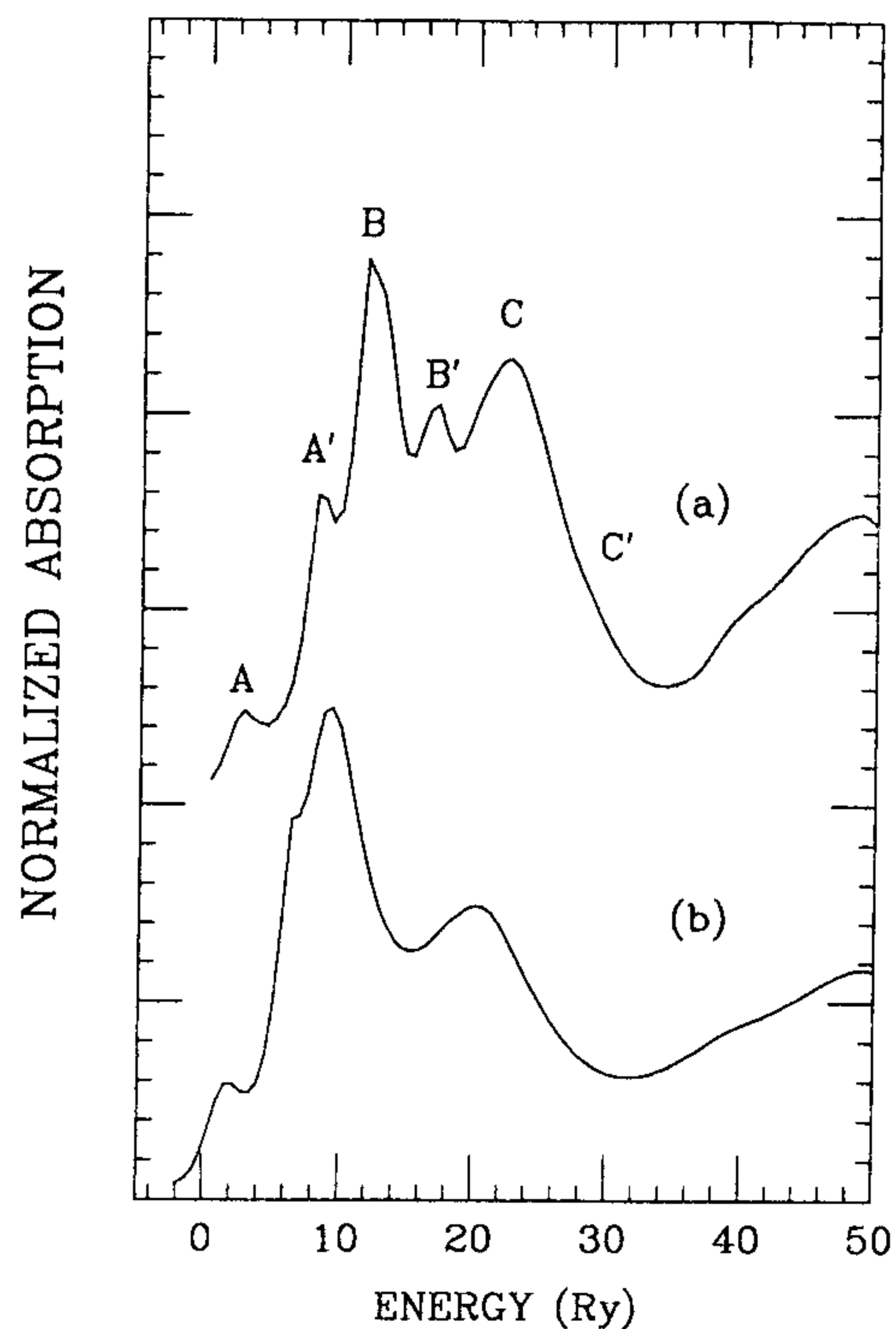


FIG. 3. Same calculations as for Fig. 2 for the  $\text{Ca}_2\text{CuO}_3$  compound.

atomic cluster used in the calculations includes 101 atoms with a radius of about 7 Å. The point group symmetry is  $D_{4h}$ , and the first shell consists of an elongated octahedron with two different Cu-O bond lengths: 1.89 Å for the four

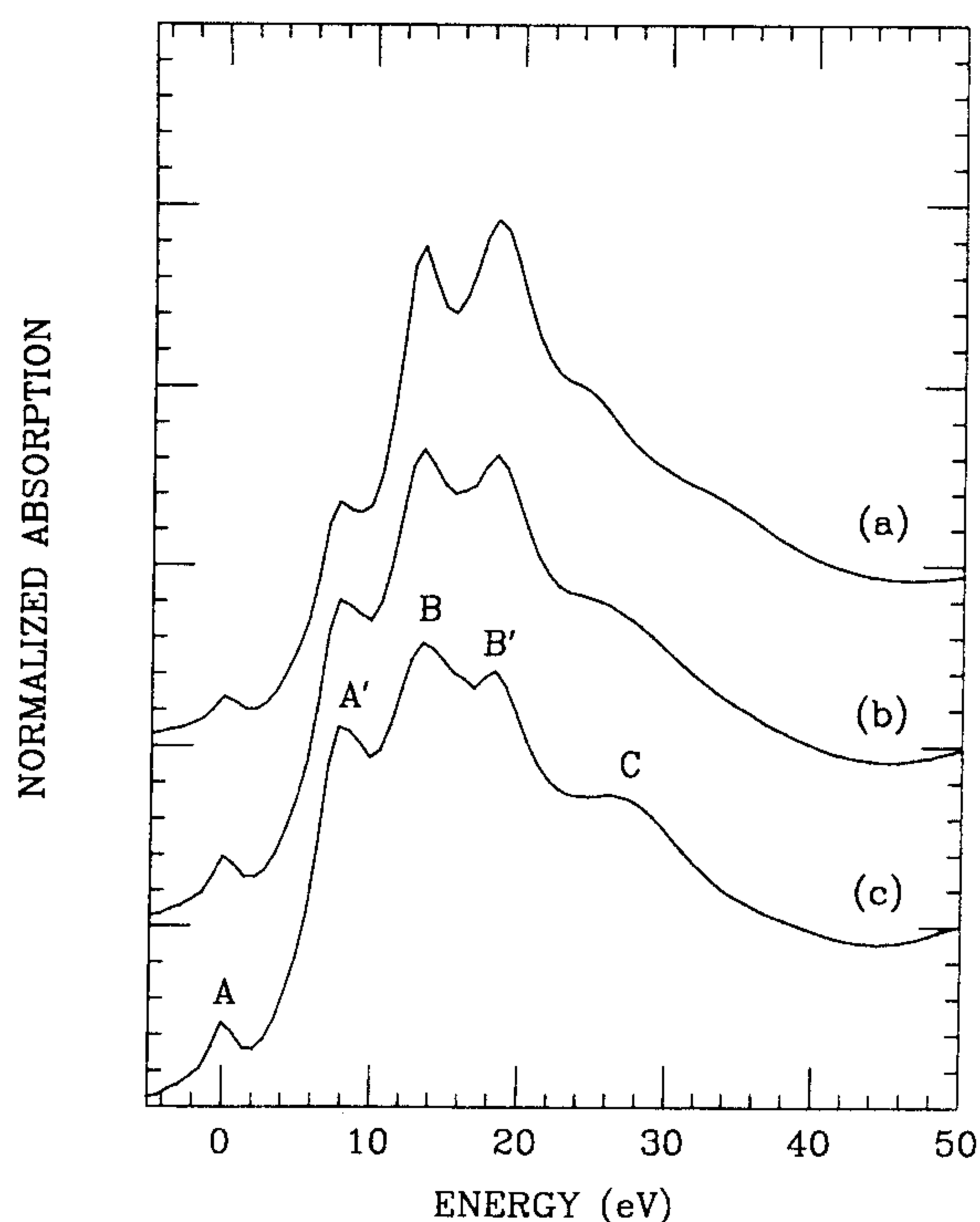


FIG. 4. Comparison between calculated XANES spectra at the Cu  $K$  edge in the  $\text{La}_2\text{CuO}_4$  compound obtained by using different weights in Eq. (1); curve (a):  $a_f^2=b_f^2=0.5$ ; curve (b):  $a_f^2=0.8$ ,  $b_f^2=0.2$ ; and curve (c):  $a_f^2=1.0$ ,  $b_f^2=0.0$ .

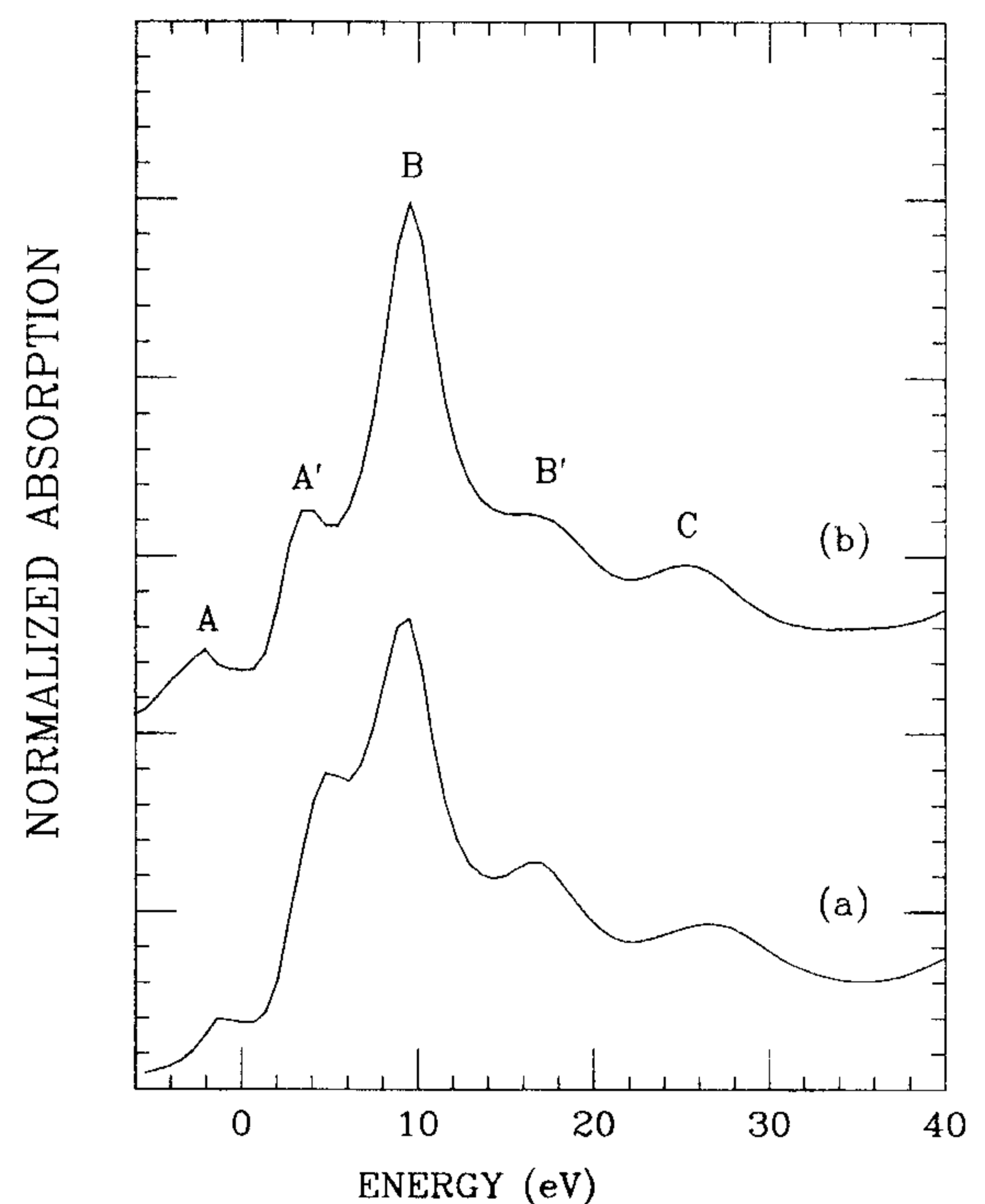


FIG. 5. Comparison between two calculations at the Cu  $K$  edge in  $\text{La}_2\text{CuO}_4$  compounds obtained by using atomic clusters within a distance of 5.8 Å from the absorber. Curve (a) refers to the case of 61 atoms.

shorter and 2.4 Å for the two longer bonds.<sup>29</sup> The three calculations are made on the basis of different percentages of the electronic configuration, mixing in the final state as indicated in the figure caption. Looking at curve (c), we observe a reasonably good agreement between experimental and theoretical spectra, although it corresponds to the calculation obtained by using only the  $3d^{10}\underline{L}$  configuration. The twin-peak structure of the spectrum, and both the relative intensity and energy position of the different features are reasonably well reproduced. The contribution coming from the  $3d^9$  configuration makes the agreement between theoretical and experimental data worse, as clearly indicated by curves (a) and (b), especially for what concerns the relative intensity of peaks B and B'.

To obtain a deeper insight into the origin of the second peak B', we have performed several calculations, changing both cluster size and geometrical arrangement around the copper central atom. For brevity, in Fig. 5, we report only the comparison between two calculations obtained by using 61 atoms [curve (a)] and 59 atoms [curve (b)] within a distance of 5.8 Å from the absorber. This last case refers to a cluster obtained by removing the two apical oxygens from the first coordination shell. The two curves are very similar, and both show the presence of a weak structure around 18 eV that becomes peak B' as we increase the number of shells in the calculation. This peak therefore appears to be an effect of atoms farther than 5.8 Å. Although our calculations seems to point to a complete structural origin of peak B', we are rather reluctant to conclude that there is no contribution of the  $3d^9$  configuration to the photoabsorption cross section of the  $\text{La}_2\text{CuO}_4$  compound, contrary to the previous two cases. In fact we believe that the admixture coefficients should be

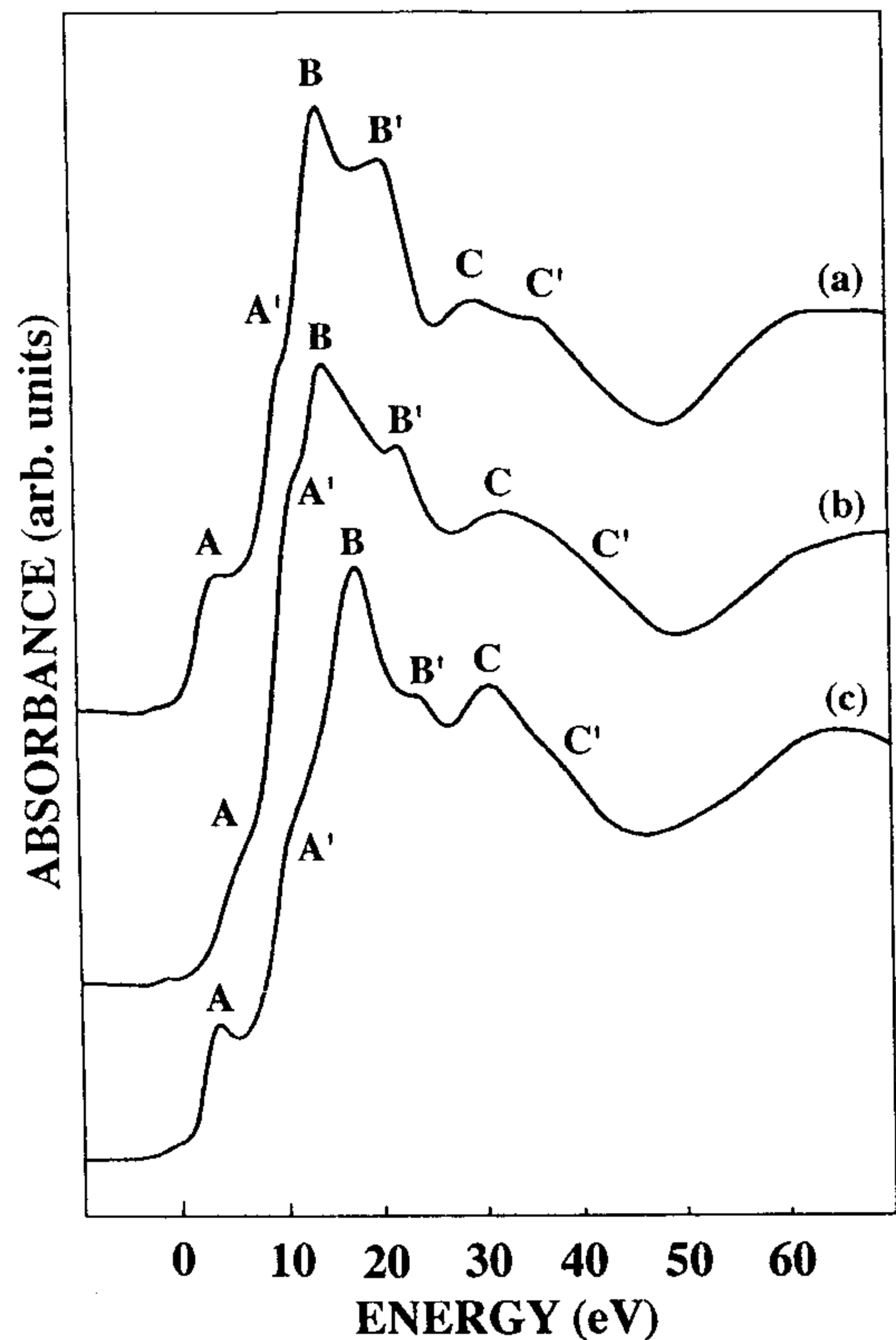


FIG. 1. Experimental data of  $\text{Nd}_2\text{CuO}_4$  [curve (a)],  $\text{La}_2\text{CuO}_4$  [curve (b)], and  $\text{Ca}_2\text{CuO}_3$  [curve (c)] at the Cu K edge measured by N. Kosugi *et al.* The well-screened  $1s \rightarrow 4p\pi$  and  $1s \rightarrow 4p\sigma$  transitions are indicated as features A and B, respectively, together with their poorly screened companions A' and B'. Also shown is the twin structures C and C'. See text for their multiple-scattering origin. Reprinted from W. Kosuyi *et al.*, Chem. Phys. **135**, 149 (1989) with kind permission of Elsevier Science - NL, Sara Burgerharrstraat 25, 1055 KV Amsterdam, The Netherlands.

configurations in the final state. This expression corresponds to the zero order in the expansion of the total absorption cross section in terms of different channel contributions, valid when the interchannel coupling is weak enough, due to the fact that either the interchannel potential or the interchannel  $T$  matrix is small compared to the single-channel scattering path operator (see Refs. 21 and 23 for details). In order to obtain the different potentials and charge densities needed for the two configurations, we used an  $X\alpha$  SCF approach for the calculation of the ground and excited states of a small cluster around the copper site. The energy splittings between the two configurations in the final state (presence of the core hole) are about  $\Delta E = 7.2$  eV for  $\text{Ca}_2\text{CuO}_3$ ,  $\Delta E = 7.1$  eV for  $\text{La}_2\text{CuO}_4$ , and  $\Delta E = 7.4$  eV for  $\text{Nd}_2\text{CuO}_4$ . The theoretical cross sections are calculated using Hedin-Lundqvist complex potential<sup>25</sup> and the muffin-tin radii are chosen according to Norman criteria.<sup>26</sup> The spectra are further convoluted with a Lorentzian shape function to account for the core-hole lifetime and experimental resolution.

In Fig. 2 theoretical calculations of Cu K edge XANES related to  $\text{Nd}_2\text{CuO}_4$  are shown. They refer to an atomic cluster of 67 atoms around the absorber, with a radius of 5.9 Å and atomic coordinates taken from Ref. 27. Locally the copper site is square coordinated with a  $D_{4h}$  point symmetry, and Cu-O bonds of about 1.97 Å. Curve (a) shows the cal-

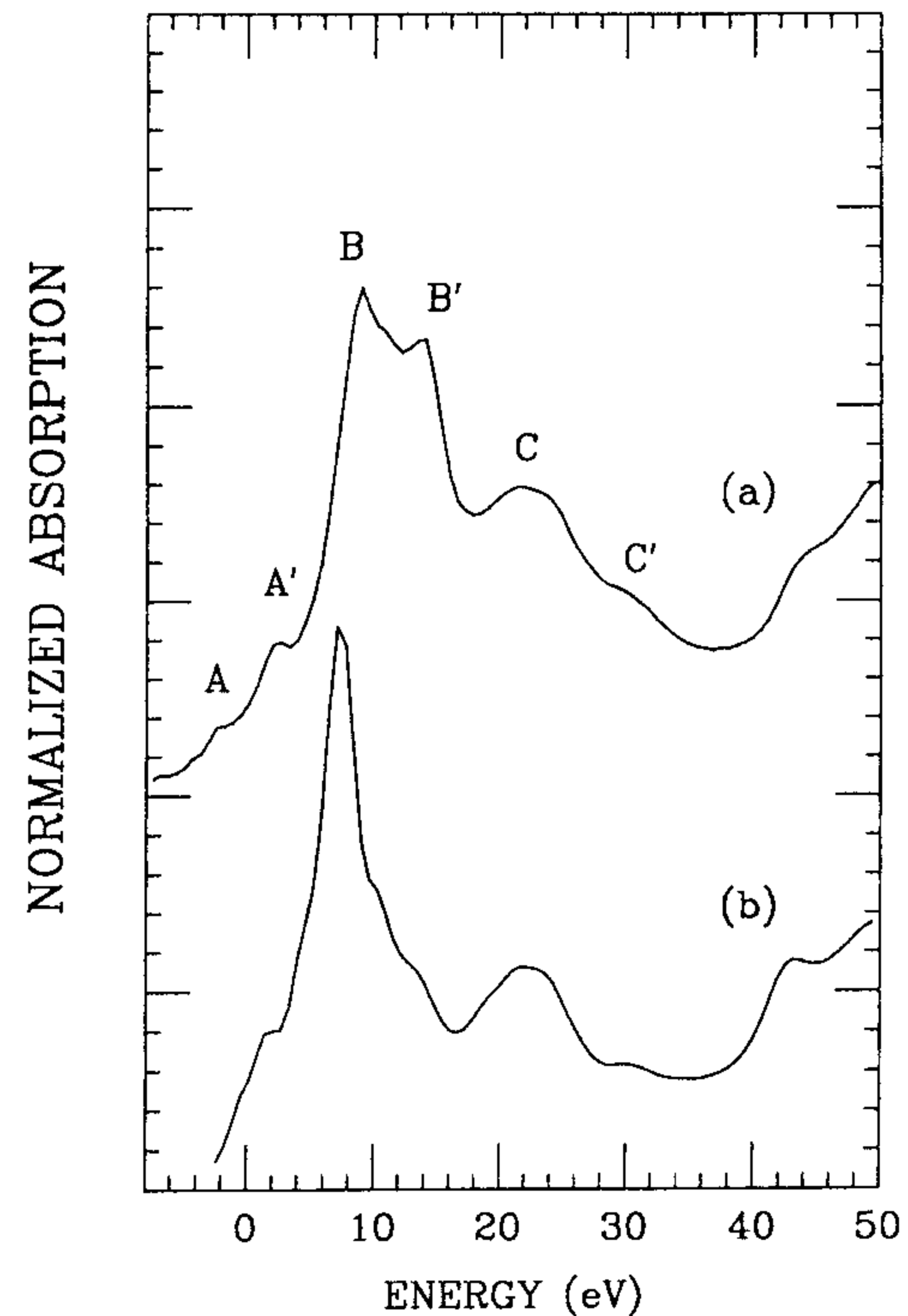


FIG. 2. Theoretical XANES spectrum at the Cu K edge in the  $\text{Nd}_2\text{CuO}_4$  compound. The calculation, based on Eq. (1) in the text, involving two configurations in the ground state, is shown in curve (a). The single-channel calculation relative to the configuration  $3d^{10}\underline{L}$  is presented in curve (b).

ulation obtained by using Eq. (1). The twin features coming from  $1s \rightarrow 4p\pi$  and  $1s \rightarrow 4p\sigma$  transitions are clearly reproduced. Good agreement between experimental data and theoretical calculations is obtained by using for the weights the following values:  $a_f^2 \approx 0.7$  and  $b_f^2 \approx 0.3$ . Also the C twin features are fairly well reproduced. In order to substantiate the presence of separate contributions coming from the two configurations, in the same figure we present [curve (b)] a theoretical calculation which uses only one configuration in the final state. Clearly the twin peak structure is not reproduced.

In Fig. 3 we present theoretical XANES spectra relative to the Cu K edge of the  $\text{Ca}_2\text{CuO}_4$  compound, which have been obtained following the same procedure described above. The first shell around the photoabsorber now forms a distorted square with two shorter Cu-O bonds of about 1.89 Å, and two longer ones of about 1.96 Å.<sup>28</sup> The atomic cluster used in the calculations consists of 69 atoms, has a radius of 6.1 Å, and a  $D_{2h}$  point-group symmetry. Curve (a) shows the calculation obtained by accounting for two final-state configurations as in the previous case. The twin-peak structure is well reproduced, and the theoretical features are in good agreement with the experimental data, both in relative intensity and energy position, by using the same relative weights for the two electronic configurations as in the case of the  $\text{Nd}_2\text{CuO}_4$  compound. For comparison we also present the calculation [curve (b)] using one electronic configuration in the final state. This calculation is in poor agreement with experimental data. Essentially a very similar behavior is observed for both  $\text{Nd}_2\text{CuO}_4$  and  $\text{Ca}_2\text{CuO}_4$  compounds.

Three different theoretical XANES spectra related to the Cu K edge of  $\text{La}_2\text{CuO}_4$  material are presented in Fig. 4. The

roughly the same in all three cases. The reason lies in the fact that the bound-state SCF calculations of a small cluster (two shells) around the Cu atom show a striking similarity between the three cases. Distribution of energy levels and energy separations between ground and excited states, and energy gaps between  $3d^{10}\underline{L}$  and  $3d^9$  electronic configurations are quite similar in the three systems. The only difference among them is that, by mere chance, the energy difference of the two structural peaks  $B$  and  $B'$  happens to be about the same energy as that of the two configurations present in the final state in the  $\text{La}_2\text{CuO}_4$  compound. As a consequence, no extra peak appears in the spectrum on which to assess the contribution of the  $3d^9$  configuration. Its amplitude can only be judged on the basis of relative intensity comparison between theoretical and experimental features present in the spectrum. This circumstance complicates the analysis, since it should be remembered that Eq. (1) is just the zero-order expansion of the total cross section in term of different contributions coming from different channels;<sup>21-23</sup> i.e., it does not account for interchannel interference. When two channels happen to interfere at a certain energy, as is the case for the  $\text{La}_2\text{CuO}_4$  compound, then our simple approximation is inadequate. Therefore a more detailed analysis of this case

must await a future implementation of interchannel interference in our computer codes.

In conclusion, by MCMS analysis we have confirmed the interpretation proposed by Kosugi *et al.*<sup>9</sup> that not all features present in the XANES spectra of the Cu  $K$  edge in  $\text{Nd}_2\text{CuO}_4$  and  $\text{Ca}_2\text{CuO}_3$  compounds have a structural origin. Indeed features  $A'$ ,  $B'$ , and  $C'$  in Fig. 1 are replicas of features  $A$ ,  $B$ , and  $C$  [which are well reproduced by a single-channel multiple-scattering (MS) calculation], due to the weighted superposition of another spectrum with a delayed onset of about 7 eV, originating from the presence of another configuration in the ground state of these compounds. However in the case of the  $\text{La}_2\text{CuO}_4$  compounds, all features appear to be well reproduced by a single-channel MS calculation relative to the  $3d^{10}\underline{L}$  configuration. Despite this finding, we believe that the mixing coefficients (MC's) of the two configurations are the same as in the previous two cases, given the similarity between the ground-state SCF calculations of the three systems. Indeed, in this latter case our simple approach to estimating the MC's breaks down due to the interference between the two channels present in the final state.

We want to thank Professor Kosugi and the other authors of Ref. 9 for their copyright permission.

<sup>1</sup>F. W. Kutzler *et al.*, Solid State Commun. **46**, 803 (1983).

<sup>2</sup>F. W. Kutzler and D. E. Ellis, Phys. Rev. B **29**, 6890 (1984).

<sup>3</sup>D. Norman *et al.*, Phys. Rev. Lett. **51**, 2052 (1983).

<sup>4</sup>J. Ghijsen *et al.*, Phys. Rev. B **38**, 11 322 (1988).

<sup>5</sup>S. H. Chou *et al.*, Phys. Rev. B **34**, 12 (1986).

<sup>6</sup>Z. Y. Wu *et al.*, Phys. Rev. B **45**, 531 (1992).

<sup>7</sup>J. Guo *et al.*, Phys. Rev. B **41**, 82 (1990).

<sup>8</sup>E. E. Alp *et al.*, Phys. Rev. B **35**, 7199 (1987).

<sup>9</sup>N. Kosugi *et al.*, Chem. Phys. **135**, 149 (1989).

<sup>10</sup>H. Tolentino, Ph.D. thesis, Universite de Paris-Sud Center d'Orsay, 1990.

<sup>11</sup>Proceedings of the International Conference M2S HTSC II, Stanford, 1989, edited by R. N. Shelton, W. A. Harrison, and N. E. Phillips [Physica C **162-164** (1989)].

<sup>12</sup>J. Teon *et al.*, Phys. Rev. B **36**, 389 (1987).

<sup>13</sup>A. Bianconi *et al.*, Z. Phys. B **67**, 307 (1987).

<sup>14</sup>F. W. Lytle *et al.*, Phys. Rev. B **37**, 1550 (1988).

<sup>15</sup>J. M. Tranquada *et al.*, Phys. Rev. B **36**, 5263 (1987).

<sup>16</sup>H. Oyanagi *et al.*, Jpn. J. Appl. Phys. **26**, L638 (1987).

<sup>17</sup>J. B. Boyce *et al.*, Phys. Rev. B **36**, 5251 (1987).

<sup>18</sup>F. Baudelet *et al.*, Z. Phys. B **69**, 141 (1987).

<sup>19</sup>D. D. Sarma, Phys. Rev. B **37**, 7948 (1988).

<sup>20</sup>K. B. Gary *et al.*, Phys. Rev. B **38**, 244 (1988).

<sup>21</sup>C. R. Natoli and M. Benfatto, *Core Level Spectroscopy in Con-*

*densed Systems, Proceedings of Tenth Taniguchi International Symposium, Kashikojima, Japan, 1987* (Springer, Berlin, 1988), pp. 184-202.

<sup>22</sup>P. A. Lee and J. B. Pendry, Phys. Rev. B **11**, 2795 (1975); C. R. Natoli *et al.*, Phys. Rev. A **22**, 1104 (1980); P. J. Durham *et al.*, Comput. Phys. Commun. **25**, 193 (1982); C. R. Natoli and M. Benfatto, J. Phys. (Paris) Colloq. **47**, C8-11 (1986); P. J. Durham, in *X-Ray Absorption*, edited by D. C. Konisberger and R. Prins, Chemical Analysis Vol. 92 (Wiley, New York, 1988), p. 72.

<sup>23</sup>C. R. Natoli, M. Benfatto, C. Brouder, M. Z. Ruiz Lopez, and D. L. Foulis, Phys. Rev. B **42**, 1944 (1990).

<sup>24</sup>M. Pedio *et al.*, Phys. Rev. B **50**, 6596 (1994).

<sup>25</sup>P. A. Lee and G. Beni, Phys. Rev. B **15**, 2862 (1977), H. Chou, J. J. Rehr, E. A. Stern, and E. R. Davidson, *ibid.* **35**, 2604 (1987); T. A. Tyson, K. O. Hodgson, C. R. Natoli, and M. Benfatto *ibid.* **46**, 5997 (1992).

<sup>26</sup>J. G. Norman, Mol. Phys. **81**, 1191 (1974).

<sup>27</sup>Hk. Muller-Buschbaum *et al.*, Z. Anorg. Allg. Chem. **414**, 76 (1975).

<sup>28</sup>Chr. L. Teske *et al.*, Z. Anorg. Allg. Chem. **379**, 243 (1970).

<sup>29</sup>R. J. Cava *et al.*, Phys. Rev. B **35**, 6716 (1987); Y. Tokura *et al.*, Nature (London) **337**, 345 (1989); P. Day *et al.*, J. Phys. C **20**, L429 (1987); G. H. Kwei and D. E. Partin, Phys. Rev. Lett. **65**, 3456 (1990).